CRYSTAL GROWTH & DESIGN

Article

pubs.acs.org/crystal

Weak Halogen Bonding in Solid Haloanilinium Halides Probed Directly via Chlorine-35, Bromine-81, and Iodine-127 NMR Spectroscopy

Published as part of the Crystal Growth & Design virtual special issue on Halogen Bonding in Crystal Engineering: Fundamentals and Applications

Robert J. Attrell, Cory M. Widdifield, Ilia Korobkov, and David L. Bryce*

Department of Chemistry and Centre for Catalysis Research and Innovation, University of Ottawa, 10 Marie Curie Private, Ottawa, Ontario, Canada

Supporting Information

ABSTRACT: A series of monohaloanilinium halides exhibiting weak halogen bonding (XB) has been prepared and characterized by ^{35}Cl, ^{81}Br, and ^{127}I solid-state nuclear magnetic resonance (SSNMR) spectroscopy in magnetic fields of up to 21.1 T. The quadrupolar and chemical shift (CS) tensor parameters for halide ions (Cl^-, Br^-, I^-) which act as electron density donors in the halogen bonds of these compounds are measured to provide insight into the possible relationship between halogen bonding and NMR observables. The NMR data for certain series of related compounds are strongly indicative of when such compounds pack in the same space group, thus providing practical structural information. Careful interpretation of the NMR data in the context of novel and previously available X-ray crystallographic data, and new gauge-including projector-augmented-wave density functional theory (GIPAW DFT) calculations has revealed several notable trends. When a series of related compounds pack in the same space group, it has been possible to interpret trends in the NMR data in terms of the strength of the halogen bond. For example, in isostructural series, the halide quadrupolar coupling constant was found to increase as the halogen bond weakens. In the case of a series of haloanilinium bromides, the ^{81}Br isotropic chemical shift and CS tensor span both decrease as the bromide−halogen XB is weakened. These trends were reproduced using both GIPAW DFT and cluster-model calculations of the bromide ion magnetic shielding tensor. Such trends are particularly exciting given the well-known role that NMR has played historically in the characterization of hydrogen bonding.

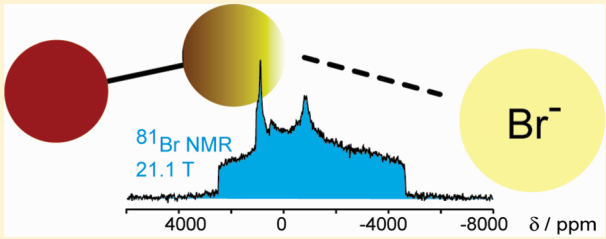

INTRODUCTION

Weak noncovalent interactions including hydrogen bonding, cation-π interactions, and halogen bonding (XB) play important roles in areas as diverse as protein and nucleic acid structure, supramolecular chemistry, and crystal engineering.[1−4] Hydrogen bonding in particular is a well-established paradigm in chemistry.[1,5] Recently, the concept of halogen bonding has garnered increased attention.[2,6−10] XB refers to a D···XY interaction where X is a halogen, D is a donor of electron density (e.g., a halide), and Y is another atom (e.g., carbon).[1] For example, Metrangolo et al. have demonstrated that iodide−iodine interactions are key to the selective capture of diiodoperfluoroalkanes by solid nonporous organic iodides.[7] Recent work by Taylor and co-workers reported on the thermodynamics of XB in solution and discussed the differences between this interaction and the hydrogen bonding interaction.[8]

NMR spectroscopy is a well-established probe of hydrogen bonding in solution and in solids, and is in fact one of the premier methods for studying these interactions.[11,12] For example, Wu et al. showed that the ^{1}H chemical shift (CS) tensor components in a series of crystalline hydrates are clearly correlated to the hydrogen bond environment[13] and have demonstrated the influence of hydrogen bonding on ^{17}O NMR interaction tensors in uracil.[14] This suggests that NMR experiments may provide equally valuable insights into halogen bonding in solids. Bouchmella et al. have presented ^{1}H, ^{13}C, and ^{15}N solid-state NMR studies of some imidazole- and morpholine-based compounds exhibiting halogen bonding capabilities.[15] However, solid-state NMR spectroscopy of $^{35/37}$Cl, $^{79/81}$Br, and ^{127}I is challenging because all of these nuclides are quadrupolar ($I > {}^1/_2$) and typically give rise to very broad powder patterns in the solid state.[16] While still far from routine, there have been significant advances in the development and application of solid-state halogen NMR spectroscopy recently. For example, we have demonstrated the sensitivity of $^{35/37}$Cl NMR parameters to the hydrogen bonding environment in amino acid hydrochlorides,[17] and of $^{79/81}$Br NMR parameters to changes in structure and hydration state.[18] The use of

Received: December 21, 2011
Published: January 6, 2012

   dx.doi.org/10.1021/cg201683p | *Cryst. Growth Des.* 2012, 12, 1641−1653

chlorine NMR to distinguish between pharmaceutical polymorphs was shown by Schurko and co-workers,[19] and the local structure around halide ions in ionic liquids was probed by Ripmeester and co-workers.[20]

Here, we report on the characterization of a series of haloanilinium halides which exhibit weak halogen bonding (Scheme 1) via $^{35/37}$Cl, $^{79/81}$Br, and ^{127}I solid-state NMR spectroscopy. The solid-state NMR spectroscopy of the covalently bound halogens (i.e., the electrophiles in halogen bonds) is generally impractical, and instead we focus our attention on the electron density donors: Cl^-, Br^-, and I^-. Semin and co-workers have reported ^{127}I nuclear quadrupole resonance (NQR) studies of covalently bound iodine atoms which are engaged in halogen bonding,[21,22] and this prompted us to explore the potential utility of examining the electron density donors involved in the halogen bonds. It has been shown recently that ^{77}Se solid-state NMR is indeed sensitive to halogen bonding with iodines in a series of selenocyanate/diiodoperfluorobenzene complexes.[23] One of the goals of the present study is therefore to explore what influence a halogen bonding interaction can have on the NMR parameters (e.g., the quadrupolar coupling constant and the chemical shift tensors) of Cl^-, Br^-, and I^- when they are electron donors in a halogen bond. The solid-state NMR studies are supported with single-crystal X-ray crystallographic studies as well as gauge-including projector-augmented-wave density functional theory (GIPAW DFT) calculations[24−27] of the relevant NMR interaction tensors.

Scheme 1. General Molecular Structure of Monohaloanilinium Halides[a]

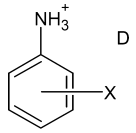

[a]X is an electron density acceptor and D is a donor of electron density. X = Cl, Br, I. D = Cl^-, Br^-, I^-.

EXPERIMENTAL SECTION

(i). Sample Preparation. All organic compounds were purchased from Sigma-Aldrich and used without further purification. The starting materials and products are air stable, and preparation was performed using a procedure adapted from the literature.[28] Synthesis consisted of mixing a given haloaniline with an excess of a given hydrohalic acid. This was followed by a period where the salt was allowed to precipitate from an ethanol solution, and the samples were filtered through a Buchner funnel with light suction and then completely dried in air at room temperature. Crystals were grown from ethanol by slow evaporation over several days, and their identities were confirmed by single-crystal X-ray diffraction. Compound numbering is given in Table 1. Crystals were powdered prior to solid-state NMR studies. Before NMR experiments, all powder samples were packed tightly into 1.3, 2.5, or 4 mm o.d. zirconium oxide magic-angle spinning (MAS) rotors.

(ii). X-ray Crystallography. Crystals of **2**, **3**, **12**, and **13** were mounted on thin glass fibers using paraffin oil and cooled to 200.15 K prior to data collection. Data were collected on a Bruker AXS SMART single crystal diffractometer equipped with a sealed Mo tube source (wavelength = 0.71073 Å) and an APEX II CCD detector. Raw data collection and processing were performed with the APEX II software package from BRUKER AXS.[29] Diffraction data were collected with a sequence of 0.5° ω scans at 0, 120, and 240° in φ. Initial unit cell parameters were determined from 60 data frames collected for

Table 1. Compound Numbering and Some Crystal Structure and Local Halogen Bonding Geometrical Information for Monohaloanilinium Halides for Which Either Single-Crystal X-ray Diffraction or Halogen Solid-State NMR Data Are Available

compound number[a]	compound name	space group	crystal structure reference	C−X (Å)	X···D (Å)[b]	C−X···D (°)	R[c]
1	2-chloroanilinium chloride	$Pca2_1$	28	1.740	3.412	170.6	0.96
2	2-bromoanilinium chloride	$Pca2_1$	this work	1.899	3.314	170.3	0.91
3	2-iodoanilinium chloride[d]	$P2_1/n$	this work	2.101	3.330	175.9	0.88
4	3-chloroanilinium chloride	$P2_1/n$	28	1.745	n/a	n/a	n/a
5	3-bromoanilinium chloride						
6	3-iodoanilinium chloride						
7	4-chloroanilinium chloride	$P2_1/c$	28,34	1.742	3.635	166.6	1.02
8	4-bromoanilinium chloride	$P2_1/c$	35,36	1.892	3.587	165.9	0.98
9	4-iodoanilinium chloride	$P2_1ab$	36	2.102	3.405	169.8	0.90
10	2-chloroanilinium bromide	$Pca2_1$	37	1.742	3.589	170.0	0.97
11	2-bromoanilinium bromide	$Pca2_1$	28	1.893	3.443	170.2	0.90
12	2-iodoanilinium bromide[d]	$P2_1/n$	this work	2.101	3.465	175.7	0.88
13	3-chloroanilinium bromide	$Pca2_1$	this work	1.742	3.838	164.7	1.03
14	3-bromoanilinium bromide	$P\bar{1}$	28	1.895	n/a	n/a	n/a
16	4-chloroanilinium bromide						
17	4-bromoanilinium bromide						
18	4-iodoanilinium bromide	$P\bar{1}$	36	2.102	3.704	158.4	0.94
19	2-chloroanilinium iodide						
20	2-bromoanilinum iodide						
21	2-iodoanilinium iodide	$P2_1/c$	28	2.101	3.692	170.2	0.88
24	3-iodoanilinium iodide	$P2_1/m$	28	2.104	3.782	174.2	0.90

[a]Compounds **15**, **22**, and **23** (i.e., 3-iodoanilinium bromide, 3-chloroanilinium iodide, and 3-bromoanilinium iodide) are not listed as we do not report NMR data for them and to our knowledge there is no information on their crystal structures. [b]Distance of shortest contact. Here, "X" is the covalently bound halogen and "D" is the anionic halide (donor of electron density); X and D may be different elements. [c]Relative XB distance, $R = d/(r_X + r_D)$, where d is the X···D distance and r_X and r_D are the van der Waals' radii of the electron density acceptor and donor, respectively. [d]Single-crystal X-ray diffraction revealed these compounds to be monohydrates.

dx.doi.org/10.1021/cg201683p | Cryst. Growth Des. 2012, 12, 1641−1653

Table 2. Crystallographic Data and Selected Data Collection Parameters for 2, 3, 12, and 13

compound	2-bromoanilinium chloride (2)	2-iodoanilinium chloride[a] (3)	2-iodoanilinium bromide[a] (12)	3-chloroanilinium bromide (13)
empirical formula	C_6H_7BrClN	C_6H_9ClINO	C_6H_9BrINO	C_6H_7BrClN
formula weight	208.49	273.49	317.95	208.49
crystal size, mm	0.32 × 0.25 × 0.21	0.21 × 0.18 × 0.18	0.23 × 0.19 × 0.16	0.22 × 0.21 × 0.18
crystal system	orthorhombic	monoclinic	monoclinic	orthorhombic
space group	$Pca2_1$ (No. 29)	$P2_1/n$ (No. 14)	$P2_1/n$ (No. 14)	$Pca2_1$ (No. 29)
Z	4	4	4	4
a, Å	15.606(2)	7.64850(10)	7.8293(2)	16.1551(5)
b, Å	5.4026(7)	6.64340(10)	6.7808(2)	5.5958(2)
c, Å	8.7865(11)	17.5487(3)	17.7752(4)	8.4538(2)
α, °	90	90	90	90
β, °	90	91.3540(10)	92.6510(10)	90
γ, °	90	90	90	90
volume, Å^3	740.80(17)	891.44(2)	942.66(4)	764.23(4)
calculated density, Mg/m^3	1.869	2.038	2.240	1.812
absorption coefficient, mm^{-1}	5.816	3.830	7.577	5.638
F(000)	408	520	592	408
Θ range for data collection, °	2.61−28.31	2.32−28.24	2.60−30.50	3.49−28.28
limiting indices	$h = \pm 20$, $k = \pm 7$, $l = \pm 11$	$h = \pm 9$, $k = \pm 8$, $l = \pm 23$	$h = \pm 11$, $k = \pm 9$, $l = \pm 25$	$h = \pm 21$, $k = \pm 6$, $l = \pm 11$
reflections collected/unique	5679/1695	9170/2167	19713/2829	8717/1871
R(int)	0.0246	0.0174	0.0230	0.0378
completeness to Θ = 28.32, %	98.5	97.9	98.0	99.1
max and min transmission	0.3747 and 0.2576	0.5456 and 0.5002	0.3769 and 0.2746	0.4302 and 0.3702
data/restraints/parameters	1695/1/82	2167/0/91	2829/0/91	1871/1/82
goodness-of-fit on F^2	1.084	1.084	1.050	1.017
final R indices [$I > 2\sigma(I)$]	$R_1 = 0.0239$, $wR_2 = 0.0614$	$R_1 = 0.0153$, $wR_2 = 0.0402$	$R_1 = 0.0170$, $wR_2 = 0.0410$	$R_1 = 0.0253$, $wR_2 = 0.0599$
R indices (all data)	$R_1 = 0.0259$, $wR_2 = 0.0623$	$R_1 = 0.0162$, $wR_2 = 0.0407$	$R_1 = 0.0182$, $wR_2 = 0.0416$	$R_1 = 0.0267$, $wR_2 = 0.0606$
absolute structure parameter	0.019(14)			0.038(9)
largest diff. peak/hole, e·Å^{-3}	0.282/−0.719	0.328/−0.839	0.622/−0.966	0.778/−0.758

[a]These compounds are monohydrates.

different sections of the Ewald sphere. Semiempirical absorption corrections based on equivalent reflections were applied.[30] Systematic absences in the diffraction data set and unit cell parameters were consistent with the orthorhombic $Pca2_1$ space group for **2** and **13** and the monoclinic $P2_1/n$ space group for **3** and **12**. Solutions for all compounds yielded chemically reasonable and computationally stable refinement results. Because of the non-centrosymmetric group and presence of heavy atoms for **2** and **13**, floating origin restraints were automatically generated during the refinement. The structures were solved by direct methods, completed with difference Fourier synthesis, and refined with full-matrix least-squares procedures based on F^2. In the structures of both compounds, the halide anions and the anilinium cations are situated in general positions. All non-hydrogen atoms were refined anisotropically with satisfactory thermal parameter values. Positions of all the hydrogen atoms were obtained from the Fourier map analysis; however, all hydrogen atoms were treated as idealized contributions. All scattering factors are contained in several versions of the SHELXTL program library, with the latest version used being 6.12.[31] Crystallographic data and selected data collection parameters are reported in Table 2.

(iii). Solid-State $^{35/37}$Cl,$^{79/81}$Br, and ^{127}I NMR. Data were acquired at the University of Ottawa using 9.4 and 11.7 T wide-bore magnets and at the National Ultrahigh-field NMR Facility for Solids in Ottawa at 21.1 T with a standard-bore magnet. Experiments at 9.4 and 11.7 T used a 4 mm Bruker HXY or HX MAS probe, while experiments at 21.1 T used a 4 mm HX MAS probe for bromine and iodine, a 4 mm static X probe for chlorine, as well as a 2.5 mm HX MAS probe for chlorine and 1.3 mm HX MAS probe for bromine. Chlorine-35/37, bromine-79/81, and iodine-127 NMR spectra were referenced to 0.1 mol/dm^3 NaCl in D_2O, 0.01 mol/dm^3 NaBr in D_2O, and 0.01 mol/dm^3 KI in D_2O, respectively. The secondary standards used were solid NaCl (−41.11 ppm) or KCl (8.54 ppm), solid KBr (54.51 ppm), and solid KI (192.62 ppm). Pulse widths (π and $\pi/2$) were determined using the secondary standard, and the selective central transition pulse scaling factors were calculated using the expression $1/(I + 1/2)$, where I is the spin quantum number of the nucleus. SSNMR signals for $^{35/37}$Cl, $^{79/81}$Br, and ^{127}I were acquired using the Solomon ($\pi/2$−$\pi/2$) and Hahn ($\pi/2$−π) echo pulse sequences. For the chlorine compounds at 9.4 and 21.1 T, spectral windows of between 250 and 1000 kHz were used, acquisition times ranged from 1 to 4 ms, and proton decoupling was used when possible. Recycle delays of 2−5 s were used, $\pi/2$ pulses were between 2.5 and 4.5 μs, and echo delays were between 36 and 80 μs. Approximately 25k to 50k transients were collected for these spectra.

For bromine and iodine, spectral windows of 2 MHz were used for all compounds, with acquisition times ranging from 180 to 301 μs. Proton decoupling was used only at 21.1 T. Recycle delays were 0.25 to 0.5 s, echo delays ranged from 20 to 40 μs, and $\pi/2$ pulse lengths ranged from 1.15 to 1.6 μs. Approximately 3k to 10k transients were collected for each piece for these spectra. Variable Offset Cumulative Spectrum (VOCS)[32] data acquisition was used when required for chlorine, bromine, and iodine. Offsets were set to 250 kHz for the $\pi/2$−$\pi/2$ and $\pi/2$−π piecewise experiments. The resulting spectra were coadded in the frequency domain to produce the final spectrum. Fast MAS (up to 62.5 kHz) was employed for some ^{81}Br NMR spectra. Note that spectra acquired for ^{37}Cl and ^{79}Br were used to confirm all spectral parameters, but the data are not shown here. SSNMR lineshapes were fit using WSolids1 simulation software that allows for analytical modeling of chemical shift anisotropy (CSA) and quadrupolar effects simultaneously.[33] All simulated spectra include only the effects of the central transition.

(iv). Quantum Chemical Calculations. GIPAW DFT (PBE exchange-correlation functional under the generalized gradient approximation) calculations of NMR parameters were performed using the CASTEP[24−27] program for all compounds for which crystal structures are available or which were solved in the course of this

dx.doi.org/10.1021/cg201683p | Cryst. Growth Des. 2012, 12, 1641−1653

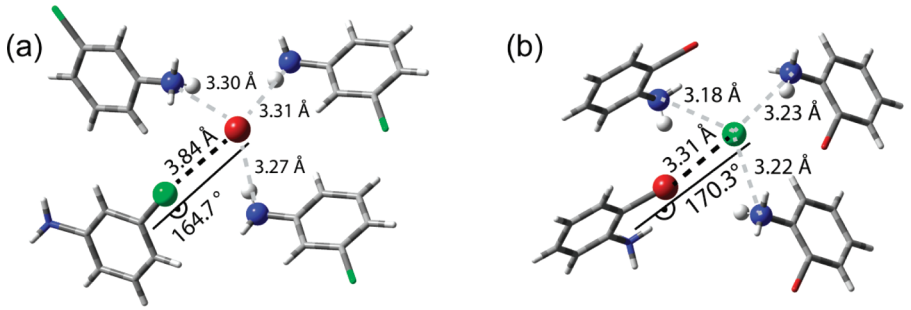

Figure 1. Important distances and angles around the halide ion in (a) 3-chloroanilinium bromide (**13**) and in (b) 2-bromoanilinium chloride (**2**). Labeled are the C−X···D angle, the halogen−halide distance, and the halide−nitrogen distances.

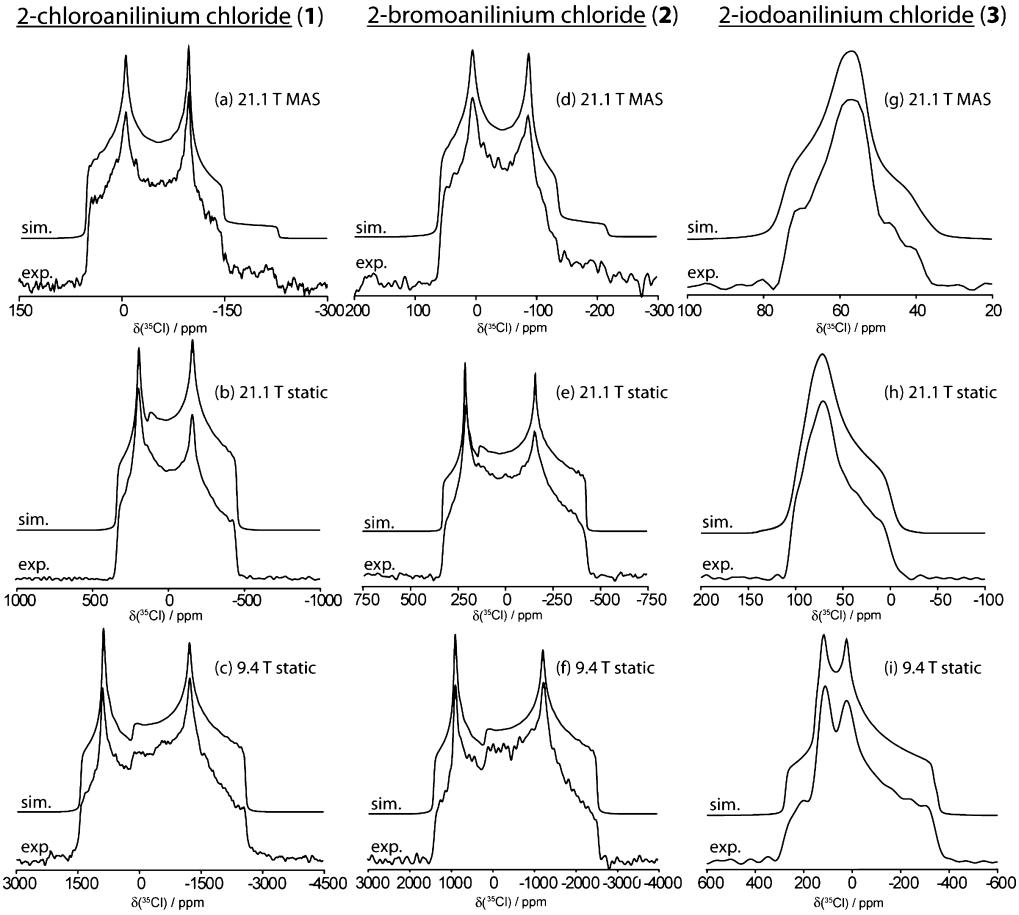

Figure 2. (a−i) Chlorine-35 SSNMR spectra of **1**, **2**, and **3**. See the Experimental section for further details on how the data were acquired and processed.

study. Experimental crystal structures for compounds **1**,[28] **2**, **4**,[28] **7**,[34] **8**,[35] **9**,[36] **10**,[37] **11**,[28] **13**, **14**,[28] and **18**[36] were used without geometry optimization, and some additional computations were also performed with optimization of the hydrogen atom positions. Ultrafine settings were used for the cutoff energies and *k*-point grids, unless calculations with those settings would not converge. In those cases the "fine" settings were used (see Supporting Information for energy cutoffs in eV and *k*-point grids used). Pseudopotential files were obtained directly from Accelrys Inc. Selected calculations were also performed on cluster models using Gaussian 09[38] (B3LYP/6-311++G**). Conversion of shielding constants to chemical shifts was carried out using the experimental absolute shielding scale for chlorine,[39] while for bromine a GIPAW DFT-computed value for KBr was used.

RESULTS AND DISCUSSION

(i). Crystal Structures. The crystal structures of 2-bromoanilinium chloride (**2**) and 3-chloroanilinium bromide (**13**) (Figure 1) were solved during the course of this study, and some relevant crystallographic and structural parameters are summarized in Tables 1 and 2. Also shown in Table 1 are the space groups and some geometrical information pertaining to the halogen bonding environment in the larger series of monohaloanilinium halides. The crystal structures of some of these compounds, as well as the topic of halogen bonding in monohaloanilinium halides, have been discussed previously, most notably by Rissanen and co-workers,[36] and by Gray and Jones.[28] We therefore focus our brief discussion of crystallographic aspects on how the data for the two new crystal

dx.doi.org/10.1021/cg201683p | *Cryst. Growth Des.* 2012, 12, 1641−1653

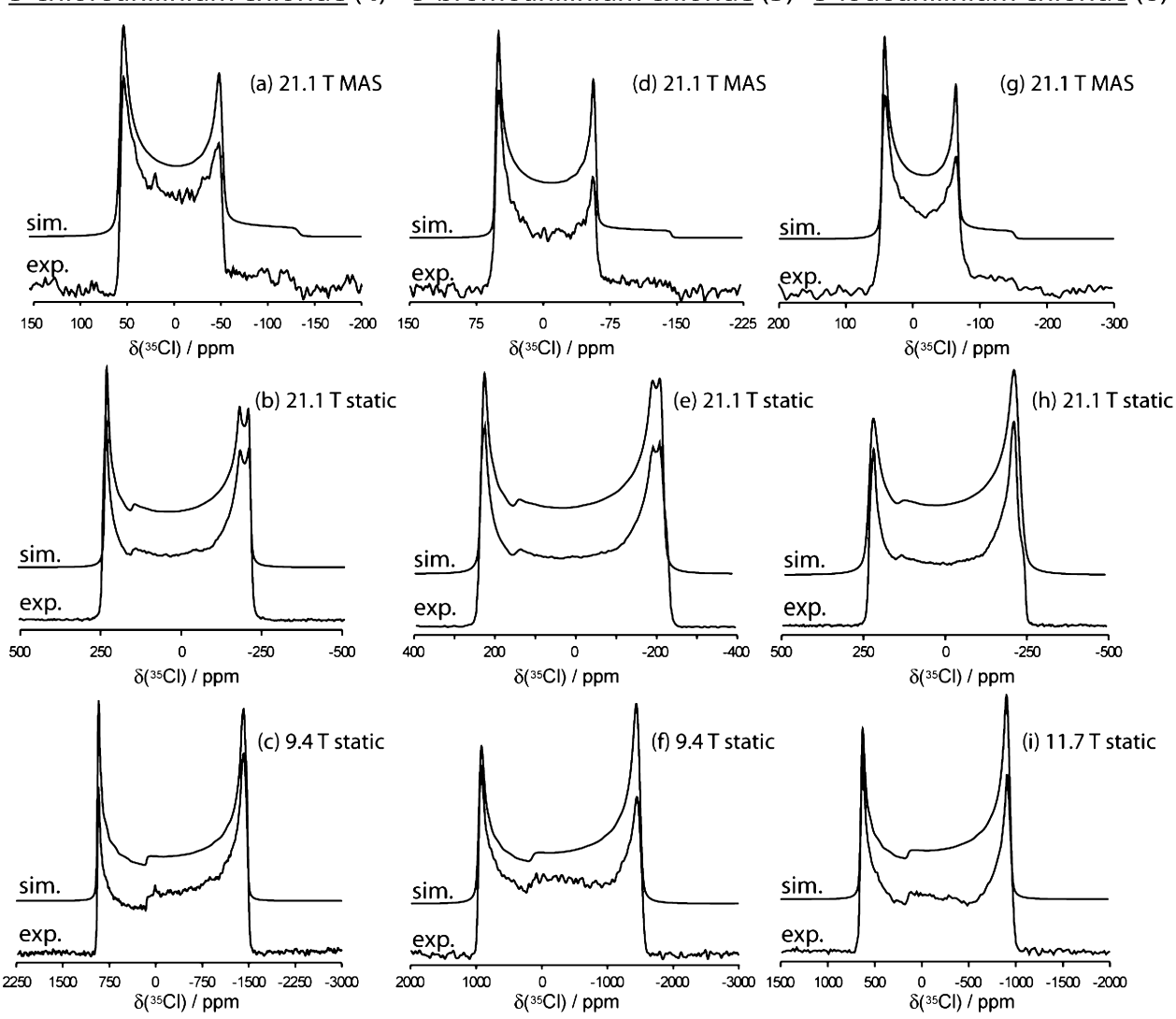

Figure 3. (a–i) Chlorine-35 SSNMR spectra of **4**, **5**, and **6**. See the Experimental section for further details on how the data were acquired and processed.

structures fit into the overall trends. This discussion also reviews relevant structural features which will be useful in the interpretation of the halogen solid-state NMR data (vide infra).

Despite the chemical similarity within the series of compounds shown in Table 1, they crystallize from ethanol in a variety of space groups. The majority of these compounds feature near-linear C–X···D angles (X = Cl, Br, I; D = Cl^-, Br^-, I^-). It is useful to discuss these contacts in terms of a normalized distance parameter, *R*,[40]

$$R = \frac{d}{r_X + r_D}$$

where *d* is the observed X···D distance, and r_X and r_D are the van der Waals' radii[41,42] of the halogen (X) and halide (D), respectively. The structures of **2** and **13** exhibit *R* values near the two extremes of all the values shown in Table 1: 0.91 for **2** and 1.03 for **13**. The latter compound, while exhibiting an approximately linear C–Cl···Br^- angle of 164.7°, therefore does not exhibit notable halogen bonding as shown by the large value of *R*. It is well-known that iodine typically forms the strongest halogen bonds within a given series.[2] The strongest halogen bonding interactions are seen for **3**, **12**, and **21** (*R* = 0.88), which is not surprising as all involve iodine as the electron density acceptor. The C–X···D angles range from 158.4° in **18** to 175.9° in **3**. The most linear contact is therefore observed when iodine is the electron density acceptor. However, overall it is clear that the halogen bonding interaction in monohaloanilinium halides is rather weak compared to the more pronounced cases observed when the electron density acceptor is *p*-diiodotetrafluorobenzene or other related perfluorinated compounds, as quantified by values of *R*. As noted previously,[28] two compounds in the series for which there are X-ray crystallographic data (**4** and **14**) do not exhibit any halogen bonding interaction; this is of interest in the context of the present study to assess whether this difference is manifested in any of the NMR parameters (vide infra).

It is important to also consider that the halide ions in these compounds are typically involved in various hydrogen bonding interactions with nearby NH groups, in addition to participating in a halogen bond. As an example, we show in Figure 1 the local halide ion environment for **2** and **13**. The interactions seen are typical of many of the compounds in

dx.doi.org/10.1021/cg201683p | *Cryst. Growth Des.* 2012, 12, 1641–1653

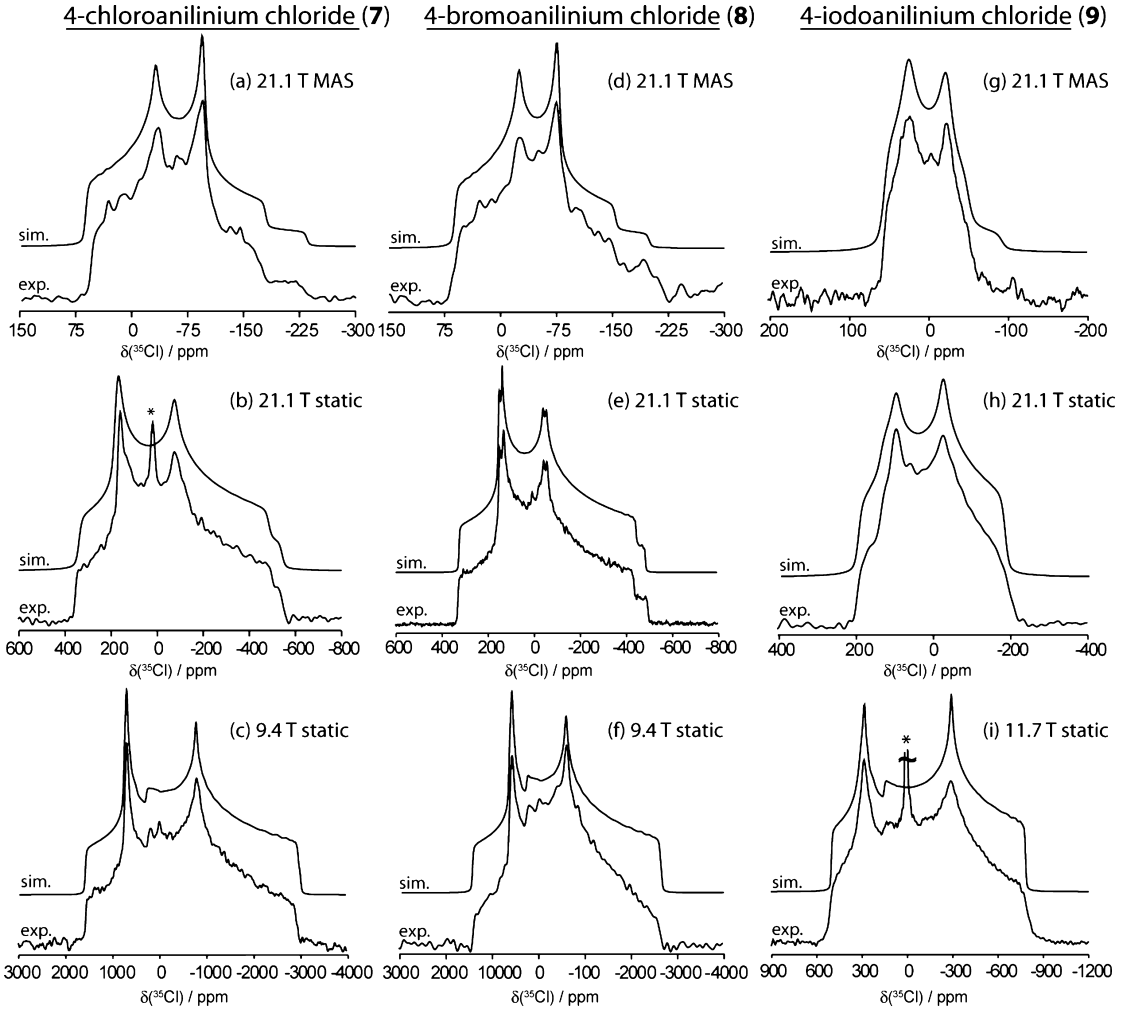

Figure 4. (a–i) Chlorine-35 SSNMR spectra of **7**, **8**, and **9**. The asterisks in (b) and (i) denote impurities. See the Experimental section for further details on how the data were acquired and processed.

Table 3. Experimental ^{35}Cl Quadrupolar and Chemical Shift Tensor Parameters[a]

compound	$\lvert C_Q(^{35}Cl)\rvert$/MHz	η_Q	δ_{iso}/ppm	Ω/ppm	κ	α (°)	β (°)	γ (°)
1	6.04(3)	0.34(1)	70(1)	95(5)	−0.20(2)	90(20)	90(5)	0(5)
2	6.01(1)	0.330(5)	79(1)	95(5)	−0.50(2)	90(20)	90(2)	0(2)
3	2.12(2)	0.76(1)	75(1)	40(5)	−0.10(2)	20(10)	85(5)	0(5)
4	5.30(5)	0.025(5)	88(1)	100(5)	−0.80(1)	0(5)	81(2)	0(2)
5	5.37(3)	0.025(5)	85(1)	95(10)	−1.0(0.1)	0(15)	83(2)	0(2)
6	5.39(5)	0.02(2)	77(1)	90(5)	−0.50(2)	0(0)	85(3)	5(3)
7	6.02(5)	0.56(1)	69(1)	115(5)	−1.0(0.1)	20(20)	90(5)	10(5)
8	5.60(5)	0.60(1)	67(1)	90(5)	−0.40(1)	75(10)	78(2)	12(2)
9	4.33(7)	0.38(1)	71(1)	120(5)	0.0(0.1)	55(10)	90(5)	0(5)

[a]Parameters are defined in terms of the principal components of the quadrupolar and CS tensors as follows: $C_Q = eQV_{33}/h$; $\eta_Q = (V_{11} - V_{22})/V_{33}$; $\delta_{iso} = (\delta_{11} + \delta_{22} + \delta_{33})/3$; $\Omega = \delta_{11} - \delta_{33}$; $\kappa = 3(\delta_{22} - \delta_{iso})/\Omega$, where $\delta_{11} \geq \delta_{22} \geq \delta_{33}$ and $|V_{11}| \leq |V_{22}| \leq |V_{33}|$. The angles α, β, γ express the relative orientation of the CS and quadrupolar tensor principal axis systems. Error bounds are in brackets. Although C_Q may take any real value, $|C_Q|$ is measured using SSNMR experiments.

Table 1 in that a single nearly linear C–X···D contact angle is present, along with three hydrogen bonds to the halide. All relevant halide–nitrogen distances are tabulated in the Supporting Information (Table 2S).

The crystal structures for compounds **3** and **12** were solved at the end of this study, as a result of the conclusions reached from our solid-state NMR studies (vide infra), and those structures will be discussed in the appropriate context below.

(ii). Chlorine-35 Solid-State NMR Spectroscopy. Presented in Figures 2, 3, and 4 are the ^{35}Cl NMR spectra of powdered samples of compounds **1**–**9**, acquired under stationary and MAS conditions. In each case, only the central transition ($m_I = {}^1/_2 \leftrightarrow -{}^1/_2$) of the ^{35}Cl nucleus in the chloride anion is observed. The ^{35}Cl quadrupolar and CS tensor parameters determined through simulation of the spectra are presented in Table 3. It is important to note that due to the

dx.doi.org/10.1021/cg201683p | Cryst. Growth Des. 2012, 12, 1641–1653

number of parameters that can influence the spectral appearance, it is advantageous to (i) acquire spectra of both stationary and MAS (where possible) samples; (ii) acquire spectra at more than one magnetic field strength; (iii) acquire spectra of another isotope when possible (i.e., ^{37}Cl in this case; data not shown). Under fast MAS conditions, the effects of CSA are removed and thus the values of the isotropic chemical shift (δ_{iso}), quadrupolar coupling constant (C_Q), and quadrupolar asymmetry parameter (η_Q) may be accurately measured (see the top row of Figures 2, 3, and 4 for ^{35}Cl MAS NMR spectra of **1**−**9**). Definitions for these NMR parameters may be found in the footnotes of Table 3. Subsequent to the proper modeling of the MAS NMR data, analysis of the NMR spectrum of a stationary sample then affords the remaining parameters. Since the line shape broadening effects of the quadrupolar interaction and the chemical shift scale differently with the applied magnetic field, acquiring data in more than one magnetic field strength increases the precision of the determined parameters.

Several important points may be made concerning the ^{35}Cl NMR spectra. Under stationary conditions, the spectra can span up to several thousand ppm at 9.4 T (see e.g., Figure 4c). By increasing the applied magnetic field strength from 9.4 to 21.1 T, the spectra narrow considerably and the signal-to-noise ratio increases. This is concomitant with the fact that the spectra are dominated by the ^{35}Cl quadrupolar interaction between the quadrupole moment of the nucleus and the electric field gradient (EFG) at the nucleus, rather than the chlorine chemical shift anisotropy. As shown in Table 3, the value of $C_Q(^{35}Cl)$ ranges from 2.12 MHz in **3** to 6.04 MHz in **1**, which fits well within the range known for hydrochloride compounds not exhibiting halogen bonding, that is, near zero to less than 10 MHz.[16] Isotropic ^{35}Cl chemical shifts for the chloride compounds range from 67 ppm in **8** to 88 ppm in **4**, and CS tensor spans range from 40 ppm in **3** up to 120 ppm in **9**. These data also fit within the known ranges for hydrochloride salts found in the literature. It is evident that there is no clear-cut NMR spectral signature for the presence of halogen bonding in these compounds. For example, attempts to correlate the NMR parameters with the degree of linearity of the halogen bond, the XB distance, or the *R* value, were unsuccessful. Even compound **4**, which does not exhibit a halogen bond, does not show particularly distinctive ^{35}Cl NMR parameters. As discussed below, however, an analysis of various trends in the NMR parameters in the context of some of the known crystal structure data reveals useful insights into how these parameters are characteristic of chloride ions which participate as halogen bond electron density donors.

The NMR spectra and data for the 2-halosubstituted compounds **1**, **2**, and **3** betray some interesting information. The crystal structures of **1** and **2** are known: both pack in the $Pca2_1$ space group and exhibit similar carbon−halogen distances and near identical halogen bond angles. There is a difference of 0.1 Å in the halogen bond length and a difference of 5% in the *R* value, with the stronger, shorter halogen bond observed for 2-bromoanilinum chloride. The ^{35}Cl NMR data are consistent with this information: the form of the second-order quadrupolar lineshapes for **1** and **2** (see Figure 2) and the corresponding quadrupolar parameters (Table 3) are identical within experimental error. The same can be said for the CS tensor span. A small difference of 9 ppm is observed for the value of $\delta_{iso}(^{35}Cl)$, however, with the larger shift observed for compound **2**, which has the stronger halogen bond. Compound **3**, however, exhibits completely different ^{35}Cl NMR spectra and ^{35}Cl quadrupolar parameters, i.e., C_Q = 2.12 MHz (vs 6.04 and 6.01 MHz for **1** and **2**) and η_Q = 0.76 (vs 0.34 and 0.330 for **1** and **2**). The span (Ω) of the chlorine CS tensor is also substantially different for **3** (40 ppm) as compared to **1** and **2** (95 ppm). This strongly implies that **3** packs in a space group other than $Pca2_1$, and indeed that the halogen and hydrogen bonding environment about the chloride ion is different from that found in the isostructural **1** and **2**. Taken together, the data for this series (**1**, **2**, and **3**) show that the NMR parameters reflect crystal symmetry and packing, and also hint that the slightly different XB environment may be reflected in the value of δ_{iso} for **1** and **2**. The value of δ_{iso} for **3** cannot be meaningfully compared to those for **1** and **2** because the quadrupolar parameters for the three compounds indicate that they pack in different space groups and therefore δ_{iso} will be affected by more than just slight differences in the XB environment in **3**.

Chlorine-35 NMR spectra for the 3-halosubstituted chloride series (**4**, **5**, and **6**) are presented in Figure 3. The spectra, as well as the NMR parameters determined through spectral simulations (Table 3), strongly imply that these three compounds pack in the same space group and exhibit similar halogen bonding geometries. Even a cursory inspection of the NMR spectra shows that they have very similar forms for the three compounds. The values of $C_Q(^{35}Cl)$ vary over a small range, from 5.30 MHz for **4** to 5.39 MHz for **6**. The quadrupolar asymmetry parameter for these three compounds is identical within experimental error (Table 3). The CS tensor parameters are also very similar for the three compounds, with small variations in δ_{iso}. Among this series, a crystal structure is only available for **4**. This compound does not exhibit halogen bonding; rather the covalently bound chlorines on adjacent molecules in the crystal structure are oriented somewhat toward each other rather than toward the halide ion. The ^{35}Cl NMR data allow us to make two important points. First, it is probable that compounds **5** and **6** are isostructural with **4**, pack in the $P2_1/n$ space group, and do not exhibit halogen bonding. Second, assessment of all of the data in Table 3 shows that the values of C_Q, δ_{iso}, and Ω for **4**, where it is known independently that halogen bonding is absent, do not appear to be unequivocally sensitive to halogen bonding such that its presence or absence may be inferred simply by the value of one of these parameters.

The 4-halosubstituted chlorides (i.e., **7**, **8**, and **9**) all have known X-ray crystal structures; **7** and **8** pack in the same space group and exhibit similar close contacts around the chloride ion, while **9** packs in a different space group (Table 1). This is distinctly reflected in the form of their ^{35}Cl NMR spectra (Figure 4) and in the values of $C_Q(^{35}Cl)$ and η_Q. For example, η_Q = 0.56 for **7**, 0.60 for **8**, and 0.38 for **9**. Compound **7** does not feature a significant halogen bond, as quantified by the *R* value of 1.02, while **8** features a long, weak halogen bond (*R* = 0.98) and **9** features a slightly more substantial halogen bond (*R* = 0.90). The small difference in the value of *R* for the two isostructural compounds (**7** and **8**) is likely not enough to manifest conclusively in the value of δ_{iso}.

Overall, for the two series of chloride compounds exhibiting halogen bonding (**1**, **2**, **3**, and **7**, **8**, **9**), it is tempting to correlate the value of $C_Q(^{35}Cl)$ with the degree of halogen bonding (as quantified by *R*). It is seen that within these two small series, larger values of C_Q tend to be observed for weaker halogen bonds. This is a tentative conclusion for various reasons: other

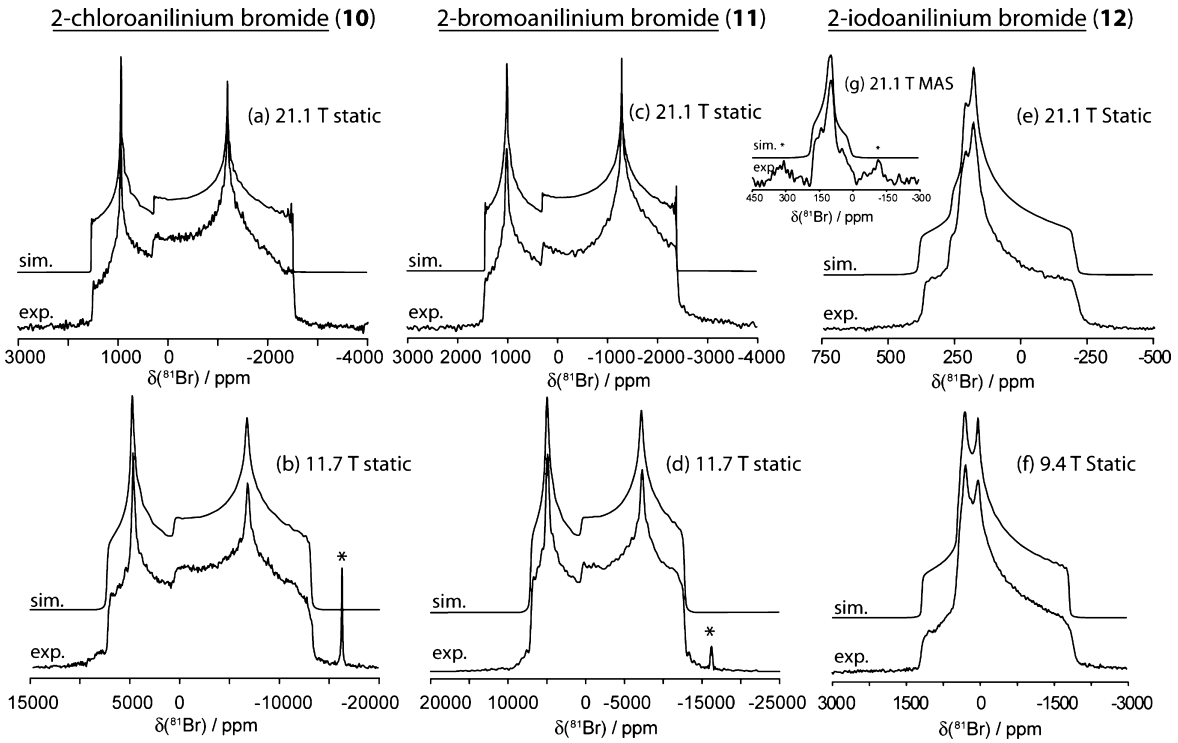

Figure 5. (a–f) Bromine-81 SSNMR spectra of **10**, **11**, and **12**. Sharp low-frequency peaks due to copper in the NMR coil are seen in (b) and (d). The MAS NMR spectrum shown in (g) is for compound **12**. See the Experimental section for further details on how the data were acquired and processed.

factors can influence C_Q, particularly when the compounds pack in different space groups. Perhaps the most important point to consider is that the hydrogen bonding environment around the chloride ions may also change from compound to compound, in addition to the halide ion bonding environment. The relevant N(H)···halogen distances are tabulated in the Supporting Information (Table 2S).

The Euler angles relating the orientations of the EFG and CS tensor principal axis systems (PAS) for these compounds consistently show that the largest components of these tensors are oriented at approximately 90 degrees to each other, as shown by the values of β in Table 3.

(iii). Bromine-81 Solid-State NMR Spectroscopy. The ^{81}Br solid-state NMR spectra of compounds **10**, **11**, **12**, **13**, **14**, **16**, and **17** are presented in Figures 5 and 6. Experimental quadrupolar and CS tensor parameters determined from spectral simulations are given in Table 4. Line shape broadening due to the quadrupolar interaction dominates the NMR spectra. The quadrupolar coupling constants, $C_Q(^{81}Br)$, range from 12.3 MHz in **12** to 45.3 MHz in **13**. Several of these values are notably larger than those obtained for other organic hydrobromides where halogen bonding is absent (i.e., $C_Q(^{81}Br)$ < 20 MHz).[20,43] The isotropic chemical shifts range from 100 ppm to 250 ppm and the CS tensor spans range from 75 ppm to 340 ppm. The isotropic chemical shifts are within the known range for bromide ions,[16] while the spans represent some of the first such data for bromide ions in organic hydrobromides.[16,18a] Interestingly, compound **14**, which does not exhibit halogen bonding, has the highest chemical shift (250 ppm) and the largest chemical shift tensor span (340 ppm).

Spectra (Figure 5) and data for the 2-halosubstituted bromide series (**10**, **11**, **12**) reflect the findings for the 2-halosubstituted chloride series (**1**, **2**, **3**), vide supra. Crystal structures are available for **10** and **11**, but not for **12**. Compounds **10** and **11** are isostructural and pack in the $Pca2_1$ space group. Both exhibit weak halogen bonding as characterized by R values of 0.97 and 0.90, respectively. The identical values of $C_Q(^{81}Br)$ of about 38 MHz for **10** and **11**, and very similar values of η_Q (0.31 and 0.27) reflect the fact that these compounds pack in the same space group. The ^{81}Br NMR spectrum and quadrupolar parameters for **12**, when contrasted with those for **10** and **11**, strongly imply that **12** is not isostructural with **10** and **11** and that it therefore packs in a different space group. Compound **11**, which exhibits a stronger halogen bond than **10**, has larger values of δ_{iso} and Ω compared with **10**. In the case of δ_{iso}, this mirrors the trend observed for the ^{35}Cl chemical shift of the isostructural chloride analogues **1** and **2** (vide supra). These observations show that isomorphism is important when attempting to investigate trends among the various compounds; otherwise, too many additional changes in the packing of the ions in the crystal can influence the observed NMR parameters.

Interestingly, the ^{81}Br NMR data for **17** clearly show the presence of two crystallographically nonequivalent bromide sites. This is the only compound in this study which exhibits two halide sites. Unfortunately, attempts to grow single crystals of **17** were unsuccessful.

(iv). Validation of Solid-State NMR Results through Additional Single-Crystal X-ray Crystallography Studies. In order to validate the findings obtained via chlorine and bromine solid-state NMR spectroscopy regarding the isomorphic nature of certain series of compounds (vide supra), the crystal structures of **3** and **12** were solved at the conclusion of this study using single-crystal X-ray diffraction. As shown in Table 1, compound **3** indeed packs in a different space group ($P2_1/n$) than do compounds **1** and **2**. This finding confirms the

dx.doi.org/10.1021/cg201683p | Cryst. Growth Des. 2012, 12, 1641–1653

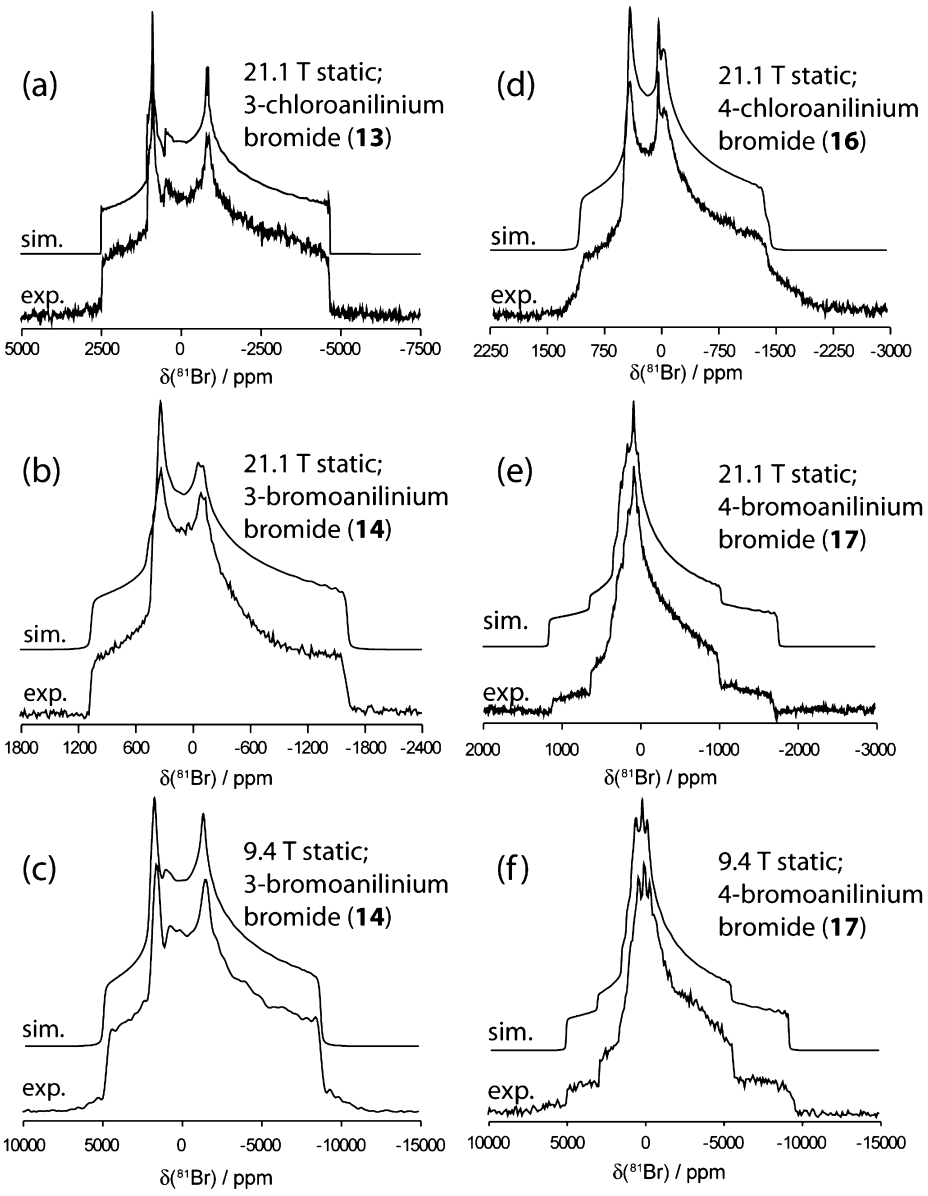

Figure 6. (a–f) Bromine-81 SSNMR spectra of **13**, **14**, **16**, and **17**. See the Experimental section for further details on how the data were acquired and processed.

Table 4. Experimental ^{81}Br Quadrupolar and Chemical Shift Tensor Parameters[a]

compound	$\lvert C_Q(^{81}Br)\rvert$/MHz	η_Q	δ_{iso}/ppm	Ω/ppm	κ	α (°)	β (°)	γ (°)
10	37.95(30)	0.31(5)	135(3)	210(20)	0.2(1)	90(25)	90(5)	0(2)
11	38.0(2)	0.27(1)	155(10)	240(10)	0.0(5)	45(2)	90(2)	0(10)
12	12.3(2)	0.85(1)	187(5)	75(10)	0.2(2)	65(3)	85(5)	0(5)
13	45.3(1)	0.665(5)	130(10)	120(30)	−0.7(2)	0(25)	75(10)	0(15)
14	27.7(2)	0.67(5)	250(10)	340(10)	−0.2(1)	90(5)	90(10)	0(2)
16	26.2(1)	0.66(1)	230(10)	220(30)	0.4(1)	90(5)	80(5)	15(10)
17 (site 1)	20.0(1)	1.0(1)	100(10)					
17 (site 2)	26.2(1)	0.92(2)	150(10)	190(20)	−1.0(1)	5(3)	10(3)	12(3)

[a]Error bounds are in brackets. Parameter definitions are in Table 3. Although C_Q may take any real value, $\lvert C_Q\rvert$ is measured using SSNMR experiments reported here.

conclusion reached by ^{35}Cl solid-state NMR. Similarly, compound **12** was also found to pack in the $P2_1/n$ space group, which is different from those of compounds **10** and **11**. This corroborates the conclusion reached by ^{81}Br solid-state NMR. **3** and **12** exhibit halogen bonding motifs analogous to **1** and **2** and to **10** and **11**; however, a water of hydration is also present in the former structures. The halide ions in **3** and **12** are therefore additionally coordinated by hydrogen bonds from these water molecules. In summary, X-ray crystallography has provided an independent cross-validation of the conclusions

dx.doi.org/10.1021/cg201683p | *Cryst. Growth Des.* 2012, 12, 1641–1653

reached regarding the packing differences in two series of compounds via halogen solid-state NMR.

(v). Iodine-127 Solid-State NMR Spectroscopy. Semin and co-workers demonstrated the existence of a frequency shift in the ^{127}I NQR spectra of fluorinated diiodoalkanes upon complexation with amines (i.e., a C−I···N halogen bonding interaction where iodine is the electron density acceptor) and also discussed how these frequency shifts may be explained using a simple molecular orbital approach.[21,22] Here, we discuss briefly the feasibility of acquiring ^{127}I solid-state NMR spectra of iodide anions, where the iodine is the halogen bond electron density donor rather than the acceptor. Iodine-127 NMR spectra are difficult to acquire due to the typically extreme spectral breadths associated with the central transition for all but the most symmetric iodide environments.[44−46] We were able to acquire spectra for compounds **19** and **20** (Figure 7).

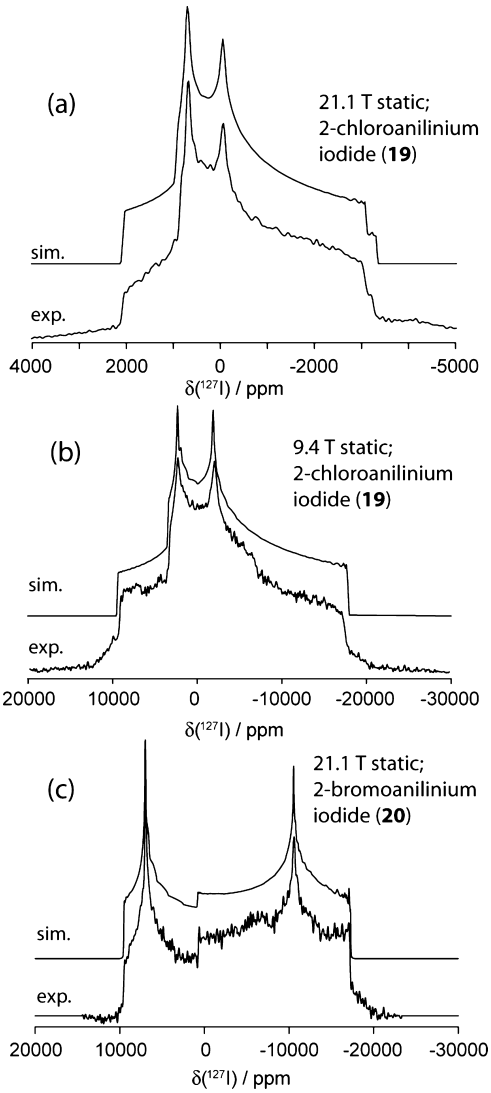

Figure 7. (a−c) Iodine-127 SSNMR spectra of **19** and **20**. See the Experimental section for further details on how the data were acquired and processed.

Note that the spectrum of **20** obtained at 21.1 T required 17 individual subspectra and that the total breadth of the central transition spectrum is on the order of 30000 ppm. Spectral parameters are presented in Table 5, where it is seen that $C_Q(^{127}I)$ is 152.50 MHz for **20**. The error inherent in the value obtained using second-order perturbation theory to fit the spectrum is estimated at less than 0.2%.[47] The distinctly different values of C_Q and η_Q for **19** and **20** strongly suggest that these two compounds are not isomorphous. Overall, the data obtained for the two compounds are consistent with the limited ^{127}I solid-state NMR data available for iodide ions in noncubic environments.[45]

The results show that, while technically challenging, ^{127}I solid-state NMR of the iodide anions involved in halogen bonds may be successfully applied in favorable cases to gain some insight into local structure and symmetry. As for chlorine and bromine, the most unambiguous interpretations of the iodine NMR data will arise when comparing data for compounds within an isostructural series.

(vi). Quantum Chemical Calculations. The results of GIPAW DFT calculations of the chlorine and bromine quadrupolar and magnetic shielding tensors are reported in Tables 6 and 7. Graphical correlations between the computed and experimental data are presented in Figure 8. We discuss the results concisely, and then apply the results to study relevant trends in the following section. The values of $C_Q(^{35}Cl)$ are consistently underestimated by the calculations. We speculate that this may be due in part to the fact that it was not computationally feasible with our resources to optimize the hydrogen atom positions prior to the calculation of the NMR parameters for all compounds. It has been shown previously that chlorine quadrupolar coupling constants in organic hydrochlorides are sensitive to the positions of nearby hydrogen atoms.[48] There is also a possibility that the halogen bonding interaction may not be adequately described using these computational methods. For instance, there has been some debate over the relative roles of dispersion, electrostatics, etc. in halogen bonds.[49] Calculated quadrupolar asymmetry parameters, CS tensor spans, and CS tensor skews are in fair to good agreement with experiment. Calculated isotropic chemical shifts are overestimated by approximately 40−50 ppm when compared to experiment. This situation could possibly be improved by using a computed absolute shielding value for the reference compound, rather than the experimental chlorine shielding scale;[39] however, this is not our preferred method as it can hide deficiencies with the computational method. Given that the hydrogen atom positions modeled onto the structures during the X-ray structure refinement process are not accurate (usually these bond lengths are too short), we optimized the hydrogen atoms computationally in cases where this was feasible. As shown in Figure 8 (data represented by crosses; values given as Supporting Information), there was no improvement in agreement with experiment for the quadrupolar coupling constant or the CS tensor span (the experimental data go from being underestimated to being overestimated), while the isotropic chemical shifts became more severely overestimated.

The computed quadrupolar coupling constants for ^{81}Br also tend to be low relative to experiment; however, the differences between experimental and calculated values are less systematic than for chlorine. The utility of these calculations in exploring trends in several NMR tensor parameters is explored in an example below.

(vii). Insight into the Halogen Bonding Environment: An Example Using a Series of Isostructural Bromides. To explore further whether insight into the XB environment around the halide ions in the haloanilinium halides may be

dx.doi.org/10.1021/cg201683p | Cryst. Growth Des. 2012, 12, 1641−1653

Table 5. Experimental ^{127}I Quadrupolar and Chemical Shift Tensor Parameters[a]

compound	$\lvert C_Q(^{127}I)\rvert$/MHz	η_Q	δ_{iso}/ppm	Ω/ppm	κ	α (°)	β (°)	γ (°)
19	57.50(75)	0.775(20)	340(10)	300(100)	−1.0(0.3)	0(0)	85(5)	25(5)
20	152.50(25)	0.235(20)	500(50)[b]	<1000	n/a	n/a	n/a	n/a

[a]Error bounds are in brackets. Parameter definitions are in Table 3. Although C_Q may take any real value, $\lvert C_Q\rvert$ is measured using SSNMR experiments. [b]Because of the large value of C_Q, an exact treatment using of the Zeeman-quadrupolar Hamiltonian, rather than second-order perturbation theory, was used for spectral simulations for **20**.

Table 6. GIPAW DFT Calculated ^{35}Cl Quadrupolar and Chemical Shift Tensor Parameters

compound	$C_Q(^{35}Cl)$/MHz	η_Q	δ_{iso}/ppm	Ω/ppm	κ	α (°)	β (°)	γ (°)
1	4.21	0.42	113.2	100.2	−0.41	49.3	85.3	7.1
2	4.25	0.54	132.1	96.2	−0.60	58.4	16.9	18.1
4	3.83	0.13	136.2	94.5	−0.65	108.1	73.4	2.1
7	3.43	0.65	124.7	74.0	−0.38	32.6	74.7	159.7
8	3.91	0.69	102.6	78.1	0.07	140.5	29.3	329.9
9	3.36	0.34	121.0	101.0	0.26	82.9	13.6	209.6

Table 7. GIPAW DFT Calculated ^{81}Br Quadrupolar and Chemical Shift Tensor Parameters

compound	$C_Q(^{81}Br)$/MHz	η_Q	δ_{iso}/ppm	Ω/ppm	κ	α (°)	β (°)	γ (°)
10	−30.94	0.61	30.9	203.9	−0.29	53.5	85.6	358.8
11	−35.49	0.23	91.4	213.5	−0.64	190.6	84.9	7.7
13	−38.17	0.87	10.3	179.8	−0.71	184.0	62.6	345.1
14	−14.48	0.68	91.5	235.7	0.22	244.5	83.6	28.7
18	−14.10	0.82	81.6	90.0	0.08	80.8	83.1	10.7

gleaned from the CS tensor, relationships between CS tensor parameters and various distances and angles characteristic of the Br^- coordination environment were assessed. Since halide ions are often involved in several weak interactions simultaneously, and as differences in crystal packing (i.e., space group) may also influence the NMR parameters, it is essential to select a subset of compounds wherein the major structural variable from compound to compound is the halide−halogen XB distance. 2-Chloroanilinium bromide, 2-bromoanilinium bromide, and 3-chloroanilinium bromide (**10**, **11**, **13**) satisfy this requirement and they all pack in the $Pca2_1$ space group. The bromide ion is involved in three hydrogen bonds whose distances are essentially invariant in these three compounds; that is, the three shortest unique Br−(H)N distances vary by only 0.03, 0.02, and 0.03 Å over the three compounds (see Supporting Information, Table 2S). The major feature that changes is the Br^-−X distance, which increases from 3.443 Å in 2-bromoanilinium bromide to 3.589 Å in 2-chloroanilinium bromide to 3.838 Å in 3-chloroanilinium bromide. As shown in Figure 9, an inverse correlation between the value of $\Omega(^{81}Br)$ and the bromide ion with the shortest halogen−halide distance is observed. The span for 3-chloroanilinium bromide, 120 ppm, is particularly valuable because the Br^-−Cl distance is comparable to the sum of their van der Waals' radii, and so this value is reflective of the limiting case of a very weak XB interaction in this series of compounds (R = 1.03). The isotropic bromine chemical shifts also follow a similar trend (Figure 9), which interestingly parallels the trend observed for ^{1}H chemical shifts in hydrogen bonds.[13]

Given the error bars on the experimental data, we set out to computationally corroborate the experimental findings and to verify that the substantial change in $\Omega(^{81}Br)$ could be correlated with a change in the halogen−halide XB length. First, the experimental trend was confirmed via GIPAW DFT calculations using the experimentally known crystal structure parameters and atomic coordinates. Computed values of $\Omega(^{81}Br)$ are of the correct order of magnitude and clearly follow the experimental trend (Figure 9). Computed bromine magnetic shielding constants also substantiate the experimental trend in bromine chemical shifts (Table 7). Second, the unit cell dimensions were adjusted by a few percent above or below the experimental values for compound **10** such that intramolecular bond distances and angles remained fixed at their experimental values, but the length of the intermolecular halogen bond was varied. The goal of these calculations was to assess as directly as possible the influence of a change in the halogen bond distance while maintaining the impact of including the full crystal lattice on the computed parameters. The trends obtained thusly are consistent with those shown in Figure 9 (see Supporting Information). As a final computational verification of the trend shown in Figure 9, a cluster model of 2-chloroanilinium bromide, which included the central bromide ion and the aromatic moieties which are involved in hydrogen and/or halogen bonding with the central ion, was built on the basis of the known atomic coordinates and the bromide−chlorine distance was systematically varied by displacing an intact haloanilinium group, while leaving the remainder of the model unchanged (see Supporting Information, Figure 3S). These B3LYP/6-311++G** results also unequivocally show that $\Omega(^{81}Br)$ and $\delta_{iso}(^{81}Br)$ decrease with decreasing XB strength (as quantified by the normalized distance parameter, R), further substantiating the experimental findings (see Supporting Information, Figure 3S).

Despite all of the above evidence, it is critical to point out that small changes in hydrogen bond lengths among **10**, **11**, and **13** (albeit an order of magnitude smaller than the changes in the XB distance; see Supporting Information, Table 2S) may also be playing an important role in the observed trends in the NMR parameters. Indeed, additional calculations (see Supporting Information, Figures 1S and 2S) show that small changes in the hydrogen bonding distances will also influence the NMR parameters in the same manner as observed experimentally.

dx.doi.org/10.1021/cg201683p | Cryst. Growth Des. 2012, 12, 1641−1653

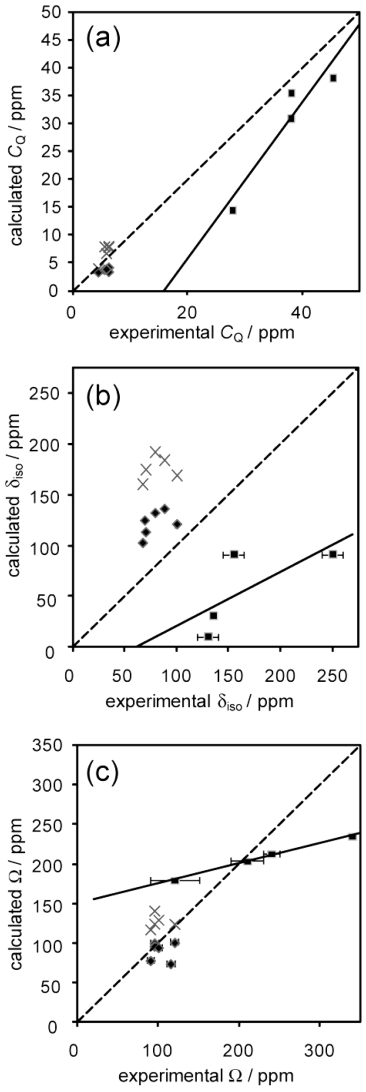

Figure 8. Comparison between (a) the experimentally determined quadrupolar coupling constants (x axis) and the GIPAW DFT-calculated values (y axis) for the compounds for which both data exist (computed data are based on experimental X-ray structures without any computational optimization). Data for six of the chloride salts are presented as filled diamond symbols (♦) and for four of the bromide salts, they are shown as filled squares. Analogous isotropic chemical shift and CS tensor span data are presented in panels (b) and (c), respectively. The lines of best fit for the bromine data are represented by solid lines. $C_Q(\text{calc}) = 1.39C_Q(\text{expt}) - 22.10$; correlation coefficient $R = 0.949$. $\Omega(\text{calc}) = 0.255\Omega(\text{expt}) + 150.3$; $R = 0.998$. $\delta_{iso}(\text{calc}) = 0.532\delta_{iso}(\text{expt}) - 33.07$; $R = 0.714$. The dashed lines represent $y = x$. Selected additional GIPAW DFT data for the chlorides are also included as crosses in each of the three panels; these values were calculated after computational optimization of the hydrogen atom positions.

Therefore, while it is not possible to conclusively attribute the changes in the bromine CS tensor in the series **10**, **11**, and **13** *solely* to changes in halogen bonding, the experimental and computational data are consistent with halogen bonding playing a role that is at least *complementary* to the role of hydrogen bonding in determining the bromide NMR parameters in these compounds. Interestingly, however, we have recently clearly shown in the case of selenium−iodine halogen bonds, in systems where hydrogen bonding is completely absent, that the chemical shift tensor span of the

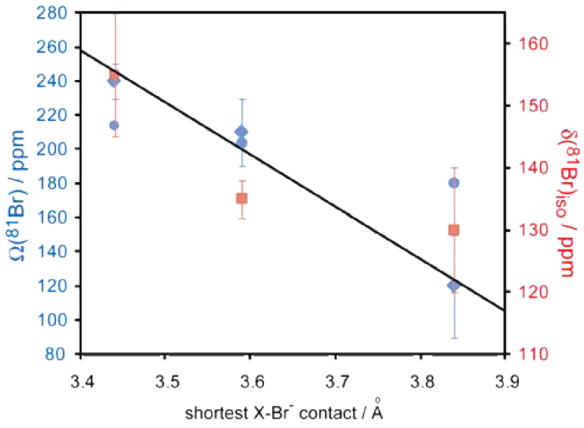

Figure 9. Plot of experimental bromine chemical shifts (red squares), bromine chemical shift tensor spans (blue diamonds), and GIPAW-DFT calculated spans (blue circles) as a function of the shortest X−Br$^-$ distance (d) in 2-chloroanilinium bromide, 2-bromoanilinium bromide, and 3-chloroanilinium bromide. The line indicates a linear fit to the experimental span data; $\Omega/\text{ppm} = -310d/(\text{Å}) + 1313$; correlation coefficient $R = 0.99$.

electron donor (selenium) is remarkably sensitive to the halogen bonding interaction.[23]

CONCLUSIONS

This study has demonstrated that it is possible to directly probe, by halogen solid-state NMR, the halide ion electron density donors in a series of halogen-bonded haloanilinium halides. Specifically, chlorine-35, bromine-81, and iodine-127 quadrupolar and chemical shift tensors have been measured for a large series of compounds exhibiting weak halogen bonding as specified by a normalized distance parameter (R values ranging from 0.88 to 1.03). The NMR data for certain series of related compounds are strongly indicative of when such compounds pack in the same space group, thereby affording useful structural information. X-ray crystallography provided an independent cross-validation of the conclusions reached regarding the packing differences in two series of compounds via halogen solid-state NMR spectroscopy.

Although we found no unequivocal halide solid-state NMR spectral signature for the presence or absence of the weak XB interaction, careful interpretation of the NMR data in the context of new and previously available crystallographic data, and new GIPAW DFT calculations, has revealed several remarkable trends. In particular, when a series of related compounds pack in the same space group, it has been possible to interpret trends in the NMR data in terms of the strength of the halogen bond. For example, in isostructural series, the halide quadrupolar coupling constant was found to increase as the halogen bond weakens. This correlation is admittedly weak for the compounds studied here. In the case of a series of haloanilinium bromide compounds, it was found that the ^{81}Br isotropic chemical shift and chemical shift tensor span both decrease as the bromide−halogen XB is weakened. These trends were reproduced using both GIPAW DFT and cluster-model calculations of the bromide ion magnetic shielding tensor. Such trends are particularly interesting given the important role which NMR has played historically in the characterization of hydrogen bonding. Future work on more strongly halogen bonded complexes will help to further generalize our findings.

dx.doi.org/10.1021/cg201683p | *Cryst. Growth Des.* 2012, 12, 1641−1653

■ ASSOCIATED CONTENT

Supporting Information

Table showing additional information on the GIPAW DFT calculations; table of relevant hydrogen bond distances; additional computational results; crystallographic information files for **2**, **3**, **12**, and **13**; complete reference 38. This material is available free of charge via the Internet at http://pubs.acs.org.

■ AUTHOR INFORMATION

Corresponding Author

*Tel: +1 613 562 5800 ext 2018. Fax: +1 613 562 5170. E-mail: dbryce@uottawa.ca.

■ ACKNOWLEDGMENTS

D.L.B. thanks the Natural Sciences and Engineering Research Council (NSERC) of Canada for funding. C.M.W. thanks NSERC for an Alexander Graham Bell CGS D2 scholarship. Dr. Victor Terskikh, Dr. Eric Ye, Dr. Glenn Facey, and Dr. Andy Lo are thanked for technical support. Access to the 900 MHz NMR spectrometer was provided by the National Ultrahigh-Field NMR Facility for Solids (Ottawa, Canada), a national research facility funded by the Canada Foundation for Innovation, the Ontario Innovation Trust, Recherche Québec, the National Research Council Canada, and Bruker BioSpin and is managed by the University of Ottawa (www.nmr900.ca). NSERC is acknowledged for a Major Resources Support grant.

■ REFERENCES

(1) Desiraju, G. R.; Steiner, T. The Weak Hydrogen Bond In Structural Chemistry and Biology. *IUCr Monographs on Crystallography*; Oxford University Press: Oxford, 1999; Vol. *9*.
(2) *Halogen Bonding: Fundamentals and Applications*; Metrangolo, P.; Resnati, G., Eds.; Mingos, D. M. P., Series Ed.; Springer-Verlag: Berlin, 2008; Structure and Bonding, Vol. *126*.
(3) Gokel, G. W.; De Wall, S. L.; Meadows, E. S. *Eur. J. Org. Chem.* **2000**, *2000*, 2967.
(4) Plevin, M. J.; Bryce, D. L.; Boisbouvier, J. *Nat. Chem.* **2010**, *2*, 466.
(5) Gilli, G.; Gilli, P. The Nature of the Hydrogen Bond: Outline of a Comprehensive Hydrogen Bond Theory. *IUCr Monographs on Crystallography*; Oxford University Press: Oxford, 2009, Vol. *23*.
(6) Metrangolo, P.; Meyer, F.; Pilati, T.; Resnati, G.; Terraneo, G. *Angew. Chem. Intl. Ed.* **2008**, *47*, 6114.
(7) Metrangolo, P.; Carcenac, Y.; Lahtinen, M.; Pilati, T.; Rissanen, K.; Vij, A.; Resnati, G. *Science* **2009**, *323*, 1461.
(8) Sarwar, M. G.; Dragisic, B.; Salsberg, L. J.; Gouliaras, C.; Taylor, M. S. *J. Am. Chem. Soc.* **2010**, *132*, 1646.
(9) Sarwar, M. G.; Dragisic, B.; Sagoo, S.; Taylor, M. S. *Angew. Chem. Intl. Ed.* **2010**, *49*, 1674.
(10) Arman, H. D.; Gieseking, R. L.; Hanks, T. W.; Pennington, W. T. *Chem. Commun.* **2010**, *46*, 1854.
(11) Grzesiek, S.; Cordier, F.; Jaravine, V.; Barfield, M. *Prog. Nucl. Magn. Reson. Spectrosc.* **2004**, *45*, 275.
(12) Aliev, A. E.; Harris, K. D. M. Probing Hydrogen Bonding in Solids Using Solid-State NMR Spectroscopy. In *Supramolecular Assembly via Hydrogen Bonds I, Structure and Bonding*; Mingos, D. M. P., Ed.; Springer-Verlag: Berlin, 2004; Vol. *108*.
(13) Wu, G.; Freure, C. J.; Verdurand, E. *J. Am. Chem. Soc.* **1998**, *120*, 13187.
(14) Ida, R.; De Clerk, M.; Wu, G. *J. Phys. Chem. A* **2006**, *110*, 1065.
(15) Bouchmella, K.; Dutremez, S. G.; Alonso, B.; Mauri, F.; Gervais, C. *Cryst. Growth Des.* **2008**, *8*, 3941.
(16) Chapman, R. P.; Widdifield, C. M.; Bryce, D. L. *Prog. Nucl. Magn. Reson. Spectrosc.* **2009**, *55*, 215.
(17) (a) Chapman, R. P.; Bryce, D. L. *Phys. Chem. Chem. Phys.* **2007**, *9*, 6219. (b) Bryce, D. L.; Sward, G. D.; Adiga, S. *J. Am. Chem. Soc.* **2006**, *128*, 2121.
(18) (a) Widdifield, C. M.; Bryce, D. L. *J. Phys. Chem. A* **2010**, *114*, 2102. (b) Widdifield, C. M.; Bryce, D. L. *Phys. Chem. Chem. Phys.* **2009**, *11*, 7120.
(19) Hamaed, H.; Pawlowski, J. M.; Cooper, B. F. T.; Fu, R.; Eichhorn, S. H.; Schurko, R. W. *J. Am. Chem. Soc.* **2008**, *130*, 11056.
(20) Gordon, P. G.; Brouwer, D. H.; Ripmeester, J. A. *Chem. Phys. Chem.* **2010**, *11*, 260.
(21) Semin, G. K.; Babushkina, T. A.; Khrlakyan, S. P.; Pervova, E. Y.; Shokina, V. V.; Knunyants, I. L. *Theor. Expt. Chem.* **1970**, *4*, 179. Translated from *Teor. Eksp. Khim.* **1968**, *4*, 275.
(22) Maksyutin, Y. K.; Babushkina, T. A.; Guryanova, Y. N.; Semin, G. K. *Theor. Chim. Acta (Berlin)* **1969**, *14*, 48.
(23) Viger-Gravel, J.; Korobkov, I.; Bryce, D. L. *Cryst. Growth Des.* **2011**, *11*, 4984.
(24) Pickard, C. J.; Mauri, F. *Phys. Rev. B* **2001**, *63*, 245101.
(25) Yates, J. R.; Pickard, C. J.; Mauri, F. *Phys. Rev. B* **2007**, *76*, 024401.
(26) Profeta, M.; Mauri, F.; Pickard, C. J. *J. Am. Chem. Soc.* **2003**, *125*, 541−548.
(27) Clark, S. J.; Segall, M. D.; Pickard, C. J.; Hasnip, P. J.; Probert, M. I. J.; Refson, K.; Payne, M. C. *Z. Kristallogr.* **2005**, *220*, 567.
(28) Gray, L.; Jones, P. G. *Z. Naturforsch.* **2002**, *57b*, 61.
(29) *APEX Software Suite v.2010*; Bruker AXS: Madison, WI, 2005.
(30) Blessing, R. *Acta Crystallogr.* **1995**, *A51*, 33.
(31) Sheldrick, G. M. *Acta Crystallogr.* **2008**, *A64*, 112.
(32) Massiot, D.; Farnan, I.; Gautier, N.; Trumeau, D.; Trokiner, A.; Coutures, J. P. *Solid State Nucl. Magn. Reson.* **1995**, *4*, 241.
(33) Eichele, K.; Wasylishen, R. E. *WSOLIDS NMR Simulation Package*, version 1.17.30; Universitat Tübingen: Germany, 2001.
(34) Ploug-Sørenson, G.; Andersen, E. K. *Acta Crystallogr.* **1985**, *C41*, 613.
(35) Portalone, G. *Acta Crystallogr. E* **2005**, *E61*, o3083.
(36) Raatikainen, K.; Cametti, M.; Rissanen, K. *Beilstein J. Org. Chem.* **2010**, *6* DOI: 10.3762/bjoc.6.4.
(37) Liu, Z.; Yu, W.-T.; Tao, X.-T.; Jiang, M.-H.; Yang, J.-X.; Wang, L. *Z. Kristallogr. NCS* **2005**, *220*, 415.
(38) Frisch, M. J. et al. *Gaussian 09*, Revision A.02; Gaussian, Inc.: Wallingford, CT, 2009.
(39) Gee, M.; Wasylishen, R. E.; Laaksonen, A. *J. Phys. Chem. A* **1999**, *103*, 10805.
(40) Lommerse, J. P. M.; Stone, A. J.; Taylor, R.; Allen, F. H. *J. Am. Chem. Soc.* **1996**, *118*, 3108.
(41) Bondi, A. *J. Phys. Chem.* **1964**, *68*, 441.
(42) Shannon, R. D. *Acta Crystallogr.* **1976**, *A32*, 751.
(43) Alonso, B.; Massiot, D.; Florian, P.; Paradies, H. H.; Gaveau, P.; Mineva, T. *J. Phys. Chem. B* **2009**, *113*, 11906.
(44) Bryce, D. L.; Widdifield, C. M.; Chapman, R. P.; Attrell, R. J. Chlorine, Bromine, and Iodine Solid-State NMR. In *NMR of Quadrupolar Nuclei in Solid Materials*; Wasylishen, R. E, Ashbrook, S. E., Wimperis, S., Eds.; John Wiley and Sons Ltd.: Chichester, UK, 2011; doi: 10.1002/9780470034590.emrstm1214
(45) Widdifield, C. M.; Bryce, D. L. *J. Phys. Chem. A* **2010**, *114*, 10810.
(46) Wu, G.; Dong, S. *Solid State Nucl. Magn. Reson.* **2001**, *20*, 100.
(47) Widdifield, C. M.; Bain, A. D.; Bryce, D. L. *Phys. Chem. Chem. Phys.* **2011**, *13*, 12413.
(48) Bryce, D. L.; Sward, G. D. *J. Phys. Chem. B* **2006**, *110*, 26461.
(49) (a) Riley, K. E.; Hobza, P. *Cryst. Growth. Des.* **2011**, *11*, 4272. (b) Riley, K. E.; Hobza, P. *J. Chem. Theory Comput.* **2008**, *4*, 232.